PHYSICAL REVIEW C **96**, 045805 (2017)

# Proton capture reaction cross section measurements on $^{162}$Er as a probe of statistical model calculations

N. Özkan,* R. T. Güray,† and C. Yalçın
*Department of Physics, Kocaeli University, Umuttepe 41380, Kocaeli, Turkey*

W. P. Tan, A. Aprahamian, M. Beard, R. J. deBoer, S. Almaraz-Calderon, S. Falahat, J. Görres, Q. Li, A. Sauerwein,‡ K. Sonnabend,‡ and M. Wiescher
*Department of Physics, University of Notre Dame, South Bend, Indiana 46556, USA*

Zs. Fülöp, Gy. Gyürky, and E. Somorjai
*MTA Atomki, P.O. Box 51, H-4001 Debrecen, Hungary*

J. Greene
*Argonne National Laboratory, Argonne, Illinois 60439, USA*

(Received 25 February 2017; revised manuscript received 23 April 2017; published 10 October 2017)

It is crucial to measure reaction cross sections relevant to the astrophysical $\gamma$ process so that theoretical reaction rates can be tested and validated with experimental data. The total cross sections for the $^{162}$Er$(p,\gamma)^{163}$Tm and the $^{162}$Er$(p,n)^{162}$Tm reactions have been measured by the activation method in center-of-mass energies from 3.973 to 8.944 MeV and from 5.962 to 8.944 MeV, respectively. The nucleus $^{162}$Er is the heaviest $p$ nuclide to be measured by the activation method using $\gamma$-ray spectroscopy, so far. It is important to note that the energy range for the $(p,\gamma)$ reaction measurement covers a large fraction of the astrophysically relevant energy region between 2.71 and 5.34 MeV. The targets were prepared by evaporating 28.2% isotopically enriched $^{162}Er_2O_3$ powder onto carbon backing foils, and bombarded with proton beams provided by the FN Tandem Accelerator at the University of Notre Dame. The reaction yields have been determined by the observed activity of produced radioactive isotopes, which was detected offline by a high-purity germanium detector. The results are presented and compared with calculations from two statistical model codes: NON-SMOKER and TALYS.

DOI: 10.1103/PhysRevC.96.045805

## I. INTRODUCTION

The synthesis of the elements heavier than iron still is not completely understood. Of these elements, most (about 99 %) are synthesized via two mechanisms [1,2]: the $s$ process and $r$ process. It was initially thought that the remaining 1%, known as $p$ nuclei, were synthesized by a third mechanism called the $p$ process. Later, however, it was recognized that there is no single process which can explain the synthesis of all $p$ nuclei. This has led to the suggestion of a number of possible subprocesses: the $rp$ process [3], the $\gamma$ process [4], the $\nu$ process [5], and the $\nu p$ process [6] (see also [7,8] and references therein). The favored scenario for synthesizing heavy $p$ nuclei ($A > 100$) is the $\gamma$ process. Characterized by a combination of photodissociation reactions on existing heavy $s$- and $r$-seed nuclei, the $\gamma$ process requires temperatures of around 2–3 $\times$ $10^9$ K [4,9]. These conditions are met in explosive stellar environments, such as the O/Ne layers of type-II supernovae [4,10] or sub-Chandrasekhar-mass type-Ia supernovae environments [11,12].

Modeling $\gamma$-process nucleosynthesis requires complex network simulations involving more than ten thousand reaction rates on about two thousand, mostly unstable, nuclei. A large number of the elements which must be included in the network calculation are proton rich and unstable. As such, they are not accessible for cross section measurements with present experimental techniques. Instead, almost all of the required rates have to be determined theoretically by means of statistical Hauser-Feshbach (HF) predictions [13]. For the HF model to be valid there needs to be sufficient level density such that the resonance spacing overlaps and the reaction can be described by averaged quantities. On the other hand, if the incident particle energy is too large the compound framework is no longer valid, preequilibrium and direct reactions start to contribute, and HF predictions cannot be applied [14–16]. There are numerous codes in the literature which have been designed to calculate statistical model cross sections. Two of the most widely used codes for nucleoastrophysics purposes are TALYS [17] and NON-SMOKER [14]. Both of these codes require a large number of HF input parameters, e.g., nuclear level density (NLD), nucleon-nucleus interaction (optical model potential, OMP), and $\gamma$-strength function (GSF). The purpose of the current paper is to test theoretical cross sections obtained from these two HF codes against new experimental

*Also at Department of Physics, University of Notre Dame, South Bend, Indiana 46556, USA; nozkan@kocaeli.edu.tr

†Also at Department of Physics, University of Notre Dame, South Bend, Indiana 46556, USA.

‡Current address: Institut für Angewandte Physik, Goethe-Universität Frankfurt, D-60438 Frankfurt am Main, Germany.

 

$^{162}$Er$(p,\gamma)$ and $^{162}$Er$(p,n)$ data as a validation of statistical model calculations for the $p$ process.

Although the $\gamma$ process has been mostly successful in explaining the production of a large range of p-nuclei, two mass regions remain problematic, $A < 124$ and $150 \leqslant A \leqslant 165$, where a number of $p$ nuclei including $^{162}$Er are underproduced [18]. Whether the origin of the problem originates from deficiencies in the astrophysical models or the statistical model and nuclear input parameters, such as the NLDs, particle OMPs, and GSF, has not as yet been clearly identified.

There has been increasing interest in measuring radiative proton capture reactions because they are the inverse of the photodisintegration reactions which comprise the $p$ process. Such measurements can be used to test the accuracy of HF predictions over the entire $p$-process mass range, and are of particular value for nuclei near closed shells where $Q$ values are low and the statistical model notoriously unreliable. It must be realized however that cross section measurements in the high mass region ($A = 162$) are hampered by severe experimental difficulties. Cross sections of radiative proton capture reactions at astrophysical energies far below the Coulomb threshold are small. In the case of the $^{162}$Er$(p,\gamma)^{163}$Tm reaction, at a typical $\gamma$-process temperature of $3 \times 10^9$ K [19] the astrophysically relevant energy region (Gamow window) is between 2.71 and 5.34 MeV. The corresponding cross section, calculated with the TALYS reaction code [17], is between $10^{-8}$ and $10^{-3}$ b respectively. The bulk of $(p,\gamma)$ measurements have been performed in the lower mass region ($A < 112$) [20–36], except for $^{120}$Te [37], $^{130}$Ba [38], and $^{152}$Gd [39]. For the $(p,n)$ channel, very few $(p,n)$ measurements have been performed, with the exception of $^{76}$Ge [20], $^{82}$Se [21], $^{85}$Rb [34], $^{120}$Te [37], $^{130}$Ba [38], and $^{152}$Gd [39]. Since the photodisintegration process $^{163}$Tm$(\gamma,p)$ directly feeds $^{162}$Er, this reaction is an excellent example for testing the reliability of the HF prediction for a higher mass region ($A \geqslant 150$); $^{163}$Tm is eligible for statistical model predictions because it has a high level density near the proton threshold [40]. Not only is the direct measurement of the photodisintegration $^{163}$Tm$(\gamma,p)^{162}$Er difficult (since the direct measurement requires photodisintegration of the short-lived radioactive isotope $^{163}$Tm), it is actually more advantageous to measure the $(p,\gamma)$ rate and derive the $(\gamma,p)$ rate with detailed balance theorem because thermal excitation is more pronounced in photodisintegration reaction rates [41]. The inverse reaction $^{162}$Er$(p,\gamma)^{163}$Tm has a $Q$ value of 3.68 MeV.

Presented in this paper are the activation measurements of the $^{162}$Er$(p,\gamma)^{163}$Tm and $^{162}$Er$(p,n)^{162}$Tm reaction cross sections. $^{162}$Er is the highest mass $p$ nucleus to have been measured via the activation method using $\gamma$-ray spectroscopy so far. The measurements have been performed at laboratory energies of 4–9 MeV as a test of the statistical model calculations over a broader energy region. Even though for the present experiment the lowest measurable cross section was around $10^{-5}$ b, mostly due to the low enrichment of $^{162}$Er isotope (28.2%) in the target, the experiment still covered the upper half of the Gamow window, as indicated in Fig. 4. Details of the measurements are given in Sec. II. The measured cross sections, as well as the comparison to the various statistical model calculations, are presented and discussed in Sec. III. Finally, conclusions are presented in Sec. IV.

## II. MEASUREMENTS

The cross section measurements for the $^{162}$Er$(p,\gamma)^{163}$Tm and $^{162}$Er$(p,n)^{162}$Tm reactions were performed with the FN Tandem Accelerator at the University of Notre Dame Nuclear Science Laboratory (Indiana, USA) using the activation method. The method is mainly composed of two parts: the first is the production of unstable nuclei by bombarding the target with charged particles, the second is the offline determination of the reaction yield using $\gamma$-ray spectroscopy. Details of the activation method and data analysis used in this study can be found in Refs. [31,42]. Unfortunately there are some limitations for activation method measurements. The residual nucleus must have an appropriate lifetime and $\gamma$-transition intensity for the decay of the reaction product. In addition, the selection of target nucleus is limited to stable (or very long-lived) nuclei. In our case $(p,\gamma)$ and $(p,n)$ reactions on $^{162}$Er lead to $^{163}$Tm and $^{162}$Tm isotopes, respectively; half-lives and $\gamma$-emission probabilities allow cross sections to be measured with the activation method. For example, in the case of proton capture on $^{162}$Er the reaction product $^{163}$Tm is radioactive and decays to $^{163}$Er with a half-life of 1.81 h by electron capture followed by $\gamma$-ray emission with the highest emission probability of 18.6%. The related decay parameters used for the analysis are summarized in Table I.

### A. Target properties

There are six stable isotopes of natural erbium, of which $^{162}$Er has the lowest natural abundance (0.139%). Material enriched with $^{162}$Er (28.2%) was purchased in an oxide form ($Er_2O_3$) from ISOFLEX [44]. Targets were prepared at Argonne National Laboratory [45]. The oxide form of enriched $^{162}$Er (28.2%) was deposited onto a 40 $\mu$g/cm$^2$ carbon backing by an electron beam gun evaporator. Eight targets were produced with thicknesses between 65 and 130 $\mu$g/cm$^2$. Target frames were made of Ta, with 1 cm diameter holes. Target

TABLE I. Decay parameters of the $^{162}$Er + $p$ reaction products [43] and measured photopeak efficiency of the $\gamma$ transitions including coincidence summing corrections, used for the analysis.

| Reaction | Product | Half-life | $E_\gamma$ (keV) | $\gamma$ emission prob. (%) | Detection eff. (%) |
|---|---|---|---|---|---|
| $^{162}$Er$(p,\gamma)$ | $^{163}$Tm | (1.810 ± 0.005) h | 104.320 ± 0.003 | 18.6 ± 0.4 | 7.6 ± 0.4 |
| | | | 241.305 ± 0.005 | 10.9 ± 0.3 | 4.9 ± 0.3 |
| $^{162}$Er$(p,n)$ | $^{162}$Tm | (21.70 ± 0.19) min | 102.00 ± 0.03 | 17.5 ± 0.7 | 6.1 ± 0.3 |
| | | | 798.68 ± 0.05 | 8.4 ± 0.3 | 1.53 ± 0.07 |

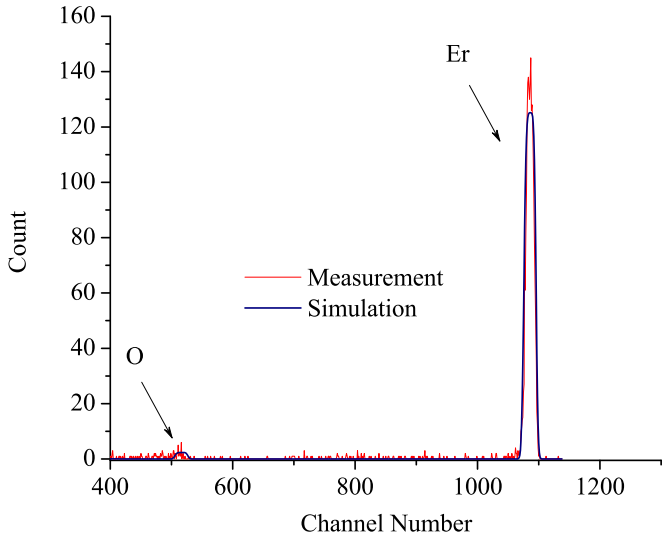


FIG. 1. A typical RBS spectrum of a target obtained with a 5 MeV $\alpha$ beam and fitted with the SIMNRA code [47].

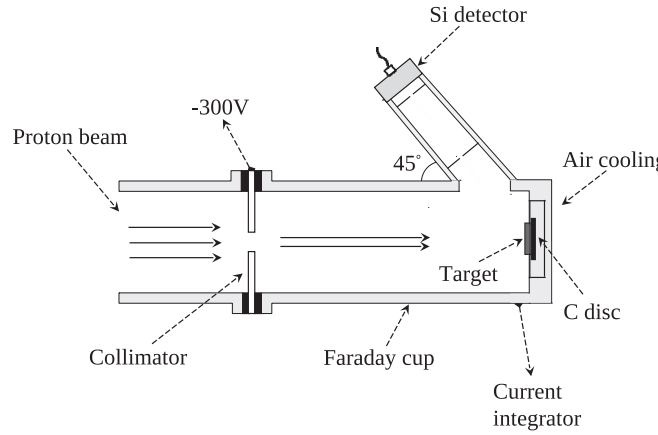


FIG. 2. A drawing of the components used in the irradiation chamber. The beam was defined by a upstream collimator with a diameter of 5 mm. The Si detector was placed at 135° with respect to beam direction for RBS measurements and checking the target stability.

thicknesses were measured by means of the energy loss of $\alpha$ particles through the target. The target was placed between a Si detector with a 1 mm diameter collimator and an $\alpha$ source in a vacuum chamber. The target thickness was deduced from the energy loss of $\alpha$ particles, emitted from a known source. By comparing the energy loss with SRIM [46] calculations, the thickness was determined. The dominant uncertainty in the thickness arises from the error in stopping power which, according to SRIM, is typically is less than 5% for $\alpha$'s. In order to determine the inhomogeneity of the thickness, the collimator was moved over the target surface. It was verified that the target thickness was inhomogeneous to within 9%. Including inhomogeneity of the target thickness, the quadratic sum of the uncertainties in the thickness is about 10%.

The target thicknesses were also verified by Rutherford backscattering spectrometry (RBS). Figure 1 shows an example of the RBS spectrum obtained with a 5 MeV $\alpha$ beam for one of the targets by a Si detector at 135°. The backscattered $\alpha$'s were detected through two 1 mm collimators as shown in Fig. 2. The measured spectrum was fitted with the SIMNRA code [47] using target composition and thickness as free parameters. Additionally, the stability of the targets was checked during irradiations by monitoring the backscattered protons.

### B. Irradiation

The Tandem accelerator provided a proton beam at laboratory energies ranging from 4.0 to 9.0 MeV. The measurements were performed at nine energies in steps of 0.5 MeV at low beam energies and 1.0 MeV at higher beam energies. These beam energies correspond to effective center-of-mass energies ($E^{\rm eff}_{\rm c.m.}$) between 3.973 and 8.944 MeV. $E^{\rm eff}_{\rm c.m.}$ is the proton center-of-mass energy at which one half of the reaction yield for the entire target thickness is obtained [48,49]. For the $^{162}$Er$(p,\gamma)^{163}$Tm reaction, this energy range partially covers the Gamow window at a temperature of $3 \times 10^9$ K.

A schematic diagram of the experimental setup for the irradiation chamber, which was located at the end of the beam line and isolated from the rest of the beam line as a Faraday cup, is shown in Fig. 2. A negatively charged bias voltage of $-300$ V was applied at the entrance of the Faraday cup to suppress secondary electrons. The beam was defined by a collimator with a diameter of 5 mm. The incident beam current was determined by the charge hitting the target during the irradiation with a current integrator. It was recorded in time intervals of 5 seconds to check the beam stability and to take the beam current fluctuations into account in the analysis. The beam current was assumed to be constant over each segment because the time segments were sufficiently small with respect to the half-life of the reaction product (see Ref. [31] for details).

In order to monitor the target stability during the irradiation, a surface barrier Si detector was built at 135° relative to the beam direction to detect the backscattered protons. A thick carbon disk was placed behind the target to stop the beam. The beam stop was air cooled during the irradiation. The applied beam current throughout the irradiations was between 70 and 250 nA, depending on the ion source and transmission of the accelerator. The target was irradiated for about 6 h for the lowest proton beam energies, 4.0 and 4.5 MeV. With the increase of beam energy, the irradiation time decreased to a minimum value of 30 min because of the fact that the cross section values increase with the proton energy. After each irradiation, the target was removed from the target chamber and then transported to the offline $\gamma$ counting system in order to measure the yield of the characteristic $\gamma$ activity of the produced unstable isotopes $^{163}$Tm and $^{162}$Tm.

### C. Determination of the activity

The reaction yields were determined by the observed activity of produced radioactive isotopes. Targets were counted offline by a high-purity germanium detector of 40% relative efficiency. The whole setup was shielded by 10 cm thick lead against laboratory background, and the inner surfaces of the

lead walls were covered with 3 mm thick Cu plates. Since low cross section measurements required the use of close geometry, $\gamma$ counting were carried out at 1 cm distance from the detector end cap, and the efficiency values had to be calculated in the same close geometry. For the analysis of $^{162}$Er$(p,\gamma)^{163}$Tm reaction, the 104.32 keV and 241.305 keV transitions were used. In the case of the $^{162}$Er$(p,n)^{162}$Tm reaction, the 102.00 and 798.68 keV $^{162}$Tm $\gamma$ transitions were used. Then, the final cross section results were derived as weighted averages of the results obtained from related $\gamma$ transitions listed in Table I. Due to the fact that all $\gamma$ countings of the irradiated samples were carried out at a close geometry of 1 cm, and that the reaction products (having high mass values) decay with a lot of $\gamma$ transitions, the true coincidence summing effect is significant and cannot be ignored.

The absolute photopeak efficiency of the detection system was determined by the efficiency-ratio method using an uncalibrated $^{152}$Eu source and calibrated $^{137}$Cs, $^{60}$Co, and $^{133}$Ba sources, each at 14 cm. This method requires knowledge of the relative emission probabilities of the source of unknown activity and at least one energy to be in an energy range for which the absolute efficiency has already been determined [50,51]. The set of relative efficiency values (relative to 122 keV $\gamma$ efficiency) obtained with $^{152}$Eu source was normalized to fit in with known efficiency values obtained with $^{137}$Cs, $^{60}$Co, and $^{133}$Ba sources. The coincidence-summing effects have been neglected at 14 cm. To normalize the counts for the measurements at the 1 cm distance to the counts at the 14 cm distance, an additional irradiation was carried out at 8 MeV laboratory energy, and then the target was counted at both 14 and 1 cm. Taking into account time durations of the countings, a factor that includes geometrical and true coincidence ones was determined by taking the ratio of the count at 14 cm to the one at 1 cm for each $\gamma$ line used in the analysis. Multiplying all measurements at 1 cm distance by this factor, the detection efficiency at 14 cm distance can be used and the coincidence-summing effect is hence eliminated.

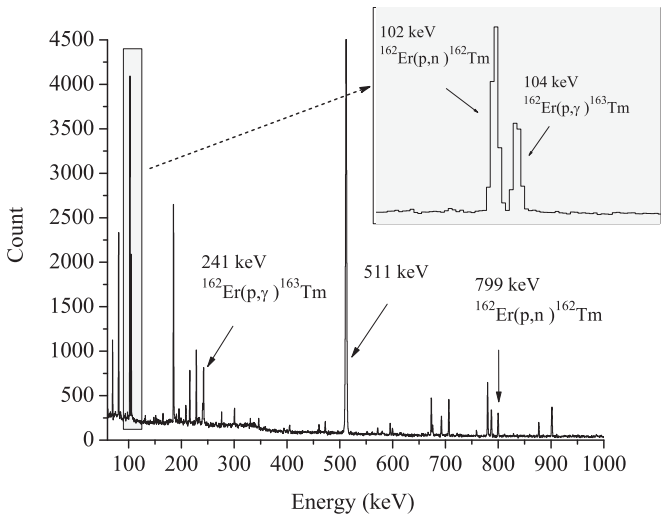


FIG. 3. A typical offline $\gamma$ spectrum after irradiating a target with 7 MeV protons. The obtained spectrum shows clearly the two resolved $\gamma$ peaks from the two reactions studied.

TABLE II. Measured cross sections and $S$ factors of the $^{162}$Er$(p,\gamma)^{163}$Tm reaction.

| $E_{beam}$ (MeV) | $E^{eff}_{c.m.}$ (MeV) | Cross section (mb) | $S$ factor ($10^{12}$ keV b) |
|---|---|---|---|
| 4 | 3.973(3) | 0.037 ± 0.005 | 60.7 ± 7.4 |
| 4.5 | 4.471(2) | 0.173 ± 0.015 | 46.5 ± 4.1 |
| 5 | 4.968(2) | 0.520 ± 0.044 | 30.3 ± 2.6 |
| 5.5 | 5.465(1) | 1.918 ± 0.158 | 30.4 ± 2.5 |
| 6 | 5.962(1) | 4.395 ± 0.362 | 22.3 ± 1.8 |
| 6.5 | 6.459(1) | 5.699 ± 0.471 | 10.7 ± 0.9 |
| 7 | 6.956(1) | 6.601 ± 0.567 | 5.1 ± 0.4 |
| 8 | 7.949(1) | 8.205 ± 0.674 | 1.40 ± 0.12 |
| 9 | 8.944(1) | 7.756 ± 0.652 | 0.38 ± 0.03 |

The photopeak efficiencies including coincidence summing corrections of the $\gamma$ transitions used for the products of the investigated reactions, $^{162}$Er$(p,\gamma)^{163}$Tm and $^{162}$Er$(p,n)^{162}$Tm, are also given in Table I.

The duration of the countings was varied between roughly 1.5 and 7 h. A typical activation $\gamma$ spectrum taken for 165 min counting time and 30 min irradiation time with a 7 MeV proton beam is shown in Fig. 3. All $\gamma$ lines used for the analysis are indicated by arrows. Many peaks coming from radioactive isotopes produced by proton induced reactions on impurities in the target and laboratory background are also visible in the spectrum, and fortunately they do not coincide with the peaks used in the analysis. The inset shows clearly the two resolved peaks (102 and 104 keV) from the two reactions studied, $(p,\gamma)$ and $(p,n)$.

## III. RESULTS AND DISCUSSION

The $^{162}$Er$(p,\gamma)^{163}$Tm and the $^{162}$Er$(p,n)^{162}$Tm reaction cross sections were measured in center-of-mass energies between 3.973 and 8.944 MeV. The purpose of these measurements is to test the statistical model cross section calculations for $^{162}$Er$(p,\gamma)$ and $^{162}$Er$(p,n)$. The experimental energy range over which the reaction cross sections were measured partially covers the Gamow window predicted for this reaction in the high temperature environment. The results obtained for the $^{162}$Er$(p,\gamma)^{163}$Tm and $^{162}$Er$(p,n)^{162}$Tm reactions are listed in Tables II and III, and graphed in Fig. 4.

The uncertainties in the cross sections are calculated by the quadratic sum of the following partial errors: target thickness

TABLE III. Measured cross sections and $S$ factors of the $^{162}$Er$(p,n)^{162}$Tm reaction.

| $E_{beam}$ (MeV) | $E^{eff}_{c.m.}$ (MeV) | Cross section (mb) | $S$ factor ($10^{12}$ keV b) |
|---|---|---|---|
| 6 | 5.962(1) | 1.1 ± 0.2 | 5.6 ± 0.9 |
| 6.5 | 6.459(1) | 8.5 ± 0.8 | 16.0 ± 1.5 |
| 7 | 6.956(1) | 21.9 ± 1.9 | 17.0 ± 1.5 |
| 8 | 7.949(1) | 70.8 ± 6.1 | 12.1 ± 1.1 |
| 9 | 8.944(1) | 154.5 ± 12.9 | 7.6 ± 0.6 |

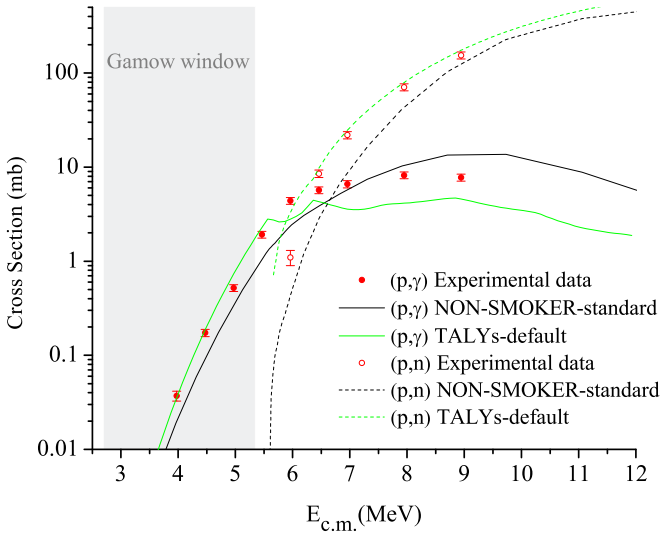


FIG. 4. Measured cross sections of the $^{162}$Er$(p,\gamma)^{163}$Tm and $^{162}$Er$(p,n)^{162}$Tm reactions compared with the HF statistical model calculations obtained with the standard settings of the statistical model code NON-SMOKER [14] and TALYS with the default parameters [17].

(10%), counting statistics (0.4% to 11%), detection efficiency with coincidence summing correction (5%), decay parameters (0.2% to $\sim$ 3%), and beam current normalization (less than 2%). The laboratory and the effective center-of-mass energies are shown in Tables II and III in the first and second columns, respectively. The effective center-of-mass energy errors are mostly due to the uncertainties in the SRIM code [52] based on the proton energy loss in the targets.

The experimental data were compared with calculations from the NON-SMOKER [14] HF code, obtained with the standard input parameter settings. The nuclear input parameters used in the NON-SMOKER code, e.g., for NLD, OMP, and GSF, are well documented and we report only brief details here. The NON-SMOKER calculations were performed with the constant temperature (CT) [53] plus backshifted Fermi gas (BSFG) model, as outlined in Ref. [13], in combination with semimicroscopic neutron and proton OMPs from Refs. [54,55]. In the NON-SMOKER code, GSFs are parametrized as either a two-Lorentzian combination, for well deformed nuclei, or one Lorentzian, for spherical and weakly deformed nuclei, according to the prescription of Ref. [56]. Figure 4 shows that the NON-SMOKER calculations are in agreement with the experimental $(p,\gamma)$ data to within a factor of 2. The NON-SMOKER calculations underestimate the experimental cross sections at low energies while overestimating at energies higher than $\sim$8 MeV. Compared to the $(p,n)$ data, the NON-SMOKER calculations underpredict the experimental cross section over the entire measured energy range: the difference goes up to a factor of 3 at low energies.

In addition, the results were also compared to calculations from the TALYS nuclear reaction code (Version 1.8) [17]. These were obtained using default TALYS input parameter settings. The CT level density prescription is the default choice in TALYS [53]. Optical model parameters are supplied by [57]. By default the OMP used in TALYS includes contributions from collective motion, where appropriate. The default choice for the GSF is the traditional standard Lorentzian model of Brink and Axel [58]. Overall, the TALYS calculations are in good agreement with the $(p,\gamma)$ data within less than a factor of 2; TALYS calculations agree well with the data at low energies while underestimating at energies higher than $\sim$6 MeV. On the other hand the TALYS predictions follow the present $(p,n)$ data well over the entire measured energy range, except at the lowest measured energy. Compared to the NON-SMOKER predictions with the standard inputs, the TALYS calculations with the default parameters provide a better overall agreement to the $(p,\gamma)$ and $(p,n)$ experimental data.

## IV. CONCLUSION

As a probe of statistical model calculations, $^{162}$Er$(p,\gamma)^{163}$Tm and $^{162}$Er$(p,n)^{162}$Tm cross sections were measured via the activation method over effective center-of-mass energy ranges of 3.973–8.944 and 5.962–8.944 MeV, respectively. The reaction channels are of particular interest for the astrophysical $p$ process, and the cross sections were measured in part over the upper end of the Gamow window. The measured cross sections were compared to statistical model calculations obtained from two widely used Hauser-Feshbach codes: NON-SMOKER [14] and TALYS [17]. Using input parameter defaults it was found that theoretical cross sections for both reaction channels agreed with the measurements to within a factor of about 2, which is in line with current expectations for statistical model calculations.

## ACKNOWLEDGMENTS

This work was supported by the EuroGENESIS research program, the Scientific and Technological Research Council of Turkey TUBITAK (108T508 and 109T585), Kocaeli University BAP (2007/36), the National Science Foundation NSF (0434844), the Joint Institute for Nuclear Astrophysics JINA (www.JINAweb.org, PHY02-16783), and The Hungarian Scientific Research Fund Programs OTKA (K108459 and K120666). A.S. and K.S. also acknowledge the financial support by DFG (SO907/2-1) and HIC for FAIR.

[1] F. Käppeler, R. Gallino, S. Bisterzo, and W. Aoki, Rev. Mod. Phys. **83**, 157 (2011).

[2] M. Arnould, S. Goriely, and K. Takahashi, Phys. Rep. **450**, 97 (2007).

[3] H. Schatz, A. Aprahamian, V. Barnard, L. Bildsten, A. Cumming, M. Ouellette, T. Rauscher, F.-K. Thielemann, and M. Wiescher, Phys. Rev. Lett. **86**, 3471 (2001).

[4] S. E. Woosley and W. M. Howard, Astrophys. J. Suppl. **36**, 285 (1978).

[5] S. E. Woosley, D. H. Hartmann, R. D. Hoffman, and W. C. Haxton, Astrophys. J. **356**, 272 (1990).

[6] C. Fröhlich, G. Martinez-Pinedo, M. Liebendörfer, F.-K. Thielemann, E. Bravo, W. R. Hix, K. Langanke, and N. T. Zinner, Phys. Rev. Lett. **96**, 142502 (2006).

[7] M. Arnould and S. Goriely, Phys. Rep. **384**, 1 (2003).

[8] T. Rauscher, N. Dauphas, I. Dillmann, C. Fröhlich, Zs. Fülöp, and Gy. Gyürky, Rep. Prog. Phys. **76**, 066201 (2013).

[9] M. Rayet, M. Arnould, M. Hashimoto, N. Prantzos, and K. Nomoto, Astron. Astrophys. **298**, 517 (1995).

[10] M. Rayet, N. Prantzos, and M. Arnould, Astron. Astrophys. **227**, 271 (1990).

[11] M. Fink, F. K. Röpke, S. A. Sim, M. Kromer, I. R. Seitenzahl, A. J. Ruiter, and W. Hillebrandt, PoS (**NIC XII**) 050 (2012).

[12] T. Rauscher, PoS (**NIC XII**) 052 (2012).

[13] T. Rauscher, F.-K. Thielemann, and K.-L. Kratz, Phys. Rev. C **56**, 1613 (1997).

[14] T. Rauscher and F. K. Thielemann, At. Data Nucl. Data Tables **75**, 1 (2000); **79**, 47 (2001); http://nucastro.org/reaclib.html.

[15] A. V. Voinov, S. M. Grimes, C. R. Brune, M. J. Hornish, T. N. Massey, and A. Salas, Phys. Rev. C **76**, 044602 (2007).

[16] J. A. Holmes, S. E. Woosley, W. A. Fowler, and B. A. Zimmerman, At. Data Nucl. Data Tables **18**, 305 (1976).

[17] A. Koning, S. Hilaire, and M. C. Duijvestijn, in *ND 2007 – International Conference on Nuclear Data for Science and Technology*, edited by O. Bersillon, F. Gunsing, E. Bauge, R. Jacqmin, and S. Leray (EDP Sciences, Les Ulis, France, 2008), p. 211; TALYS version 1.8 from http://www.talys.eu.

[18] T. Rauscher, A. Heger, R. Hoffman, and S. Woosley, Astrophys. J. **576**, 323 (2002).

[19] T. Rauscher, Phys. Rev. C **81**, 045807 (2010).

[20] G. G. Kiss, Gy. Gyürky, Z. Elekes, Zs. Fülöp, E. Somorjai, T. Rauscher, and M. Wiescher, Phys. Rev. C **76**, 055807 (2007).

[21] Gy. Gyürky, Zs. Fülöp, E. Somorjai, M. Kokkoris, S. Galanopoulos, P. Demetriou, S. Harissopulos, T. Rauscher, and S. Goriely, Phys. Rev. C **68**, 055803 (2003).

[22] Gy. Gyürky, E. Somorjai, Zs. Fülöp, S. Harissopulos, P. Demetriou, and T. Rauscher, Phys. Rev. C **64**, 065803 (2001).

[23] S. Galanopoulos, P. Demetriou, M. Kokkoris, S. Harissopulos, R. Kunz, M. Fey, J. W. Hammer, Gy. Gyürky, Zs. Fülöp, E. Somorjai, and S. Goriely, Phys. Rev. C **67**, 015801 (2003).

[24] P. Tsagari, M. Kokkoris, E. Skreti, A. G. Karydas, S. Harissopulos, T. Paradellis, and P. Demetriou, Phys. Rev. C **70**, 015802 (2004).

[25] C. E. Laird, D. Flynn, R. L. Hershberger, and F. Gabbard, Phys. Rev. C **35**, 1265 (1987).

[26] S. Harissopulos, E. Skreti, P. Tsagari, G. Souliotis, P. Demetriou, T. Paradellis, J. W. Hammer, R. Kunz, C. Angulo, S. Goriely, and T. Rauscher, Phys. Rev. C **64**, 055804 (2001).

[27] T. Sauter and F. Käppeler, Phys. Rev. C **55**, 3127 (1997).

[28] F. R. Chloupek, A. St. J. Murphy, R. N. Boyd, A. L. Cole, J. Görres, R. T. Güray, G. Raimann, J. J. Zack, T. Rauscher, J. V. Schwarzenberg, P. Tischhauser, and M. Wiescher, Nucl. Phys. A **652**, 391 (1999).

[29] J. Bork, H. Schatz, F. Käppeler, and T. Rauscher, Phys. Rev. C **58**, 524 (1998).

[30] N. Özkan, A. St. J. Murphy, R. N. Boyd, A. L. Cole, R. deHaan, M. Famiano, J. Göerres, R. T. Güray, M. Howard, L. Şahin, and M. C. Wiescher, Nucl. Phys. A **688**, 459c (2001).

[31] N. Özkan, A. St. J. Murphy, R. N. Boyd, A. L. Cole, M. Famiano, R. T. Güray, M. Howard, L. Sahin, J. J. Zack, R. deHaan, J. Görres, M. C. Wiescher, M. S. Islam, and T. Rauscher, Nucl. Phys. A **710**, 469 (2002).

[32] Gy. Gyürky, G. G. Kiss, Z. Elekes, Zs. Fülöp, E. Somorjai, and T. Rauscher, J. Phys. G: Nucl. Part. Phys. **34**, 817 (2007).

[33] M. A. Famiano, R. S. Kodikara, B. M. Giacheri, V. G. Subramanian, and A. Kayani, Nucl. Phys. A **802**, 26 (2008).

[34] G. G. Kiss, T. Rauscher, Gy. Gyürky, A. Simon, Zs. Fülöp, and E. Somorjai, Phys. Rev. Lett. **101**, 191101 (2008).

[35] A. Spyrou, A. Lagoyannis, P. Demetriou, S. Harissopulos, and H.-W. Becker, Phys. Rev. C **77**, 065801 (2008).

[36] I. Dillmann, L. Coquard, C. Domingo-Pardo, F. Käppeler, J. Marganiec, E. Uberseder, U. Giesen, A. Heiske, G. Feinberg, D. Hentschel, S. Hilpp, H. Leiste, T. Rauscher, and F.-K. Thielemann, Phys. Rev. C **84**, 015802 (2011).

[37] R. T. Güray, N. Özkan, C. Yalcin, A. Palumbo, R. deBoer, J. Görres, P. J. Leblanc, S. O'Brien, E. Strandberg, W. P. Tan, M. Wiescher, Zs. Fülöp, E. Somorjai, H. Y. Lee, and J. P. Greene, Phys. Rev. C **80**, 035804 (2009).

[38] L. Netterdon, A. Endres, G. G. Kiss, J. Mayer, T. Rauscher, P. Scholz, K. Sonnabend, Zs. Török, and A. Zilges, Phys. Rev. C **90**, 035806 (2014).

[39] R. T. Güray, N. Özkan, C. Yalçin, T. Rauscher, Gy. Gyürky, J. Farkas, Zs. Fülöp, Z. Halász, and E. Somorjai, Phys. Rev. C **91**, 055809 (2015).

[40] T. Rauscher, Phys. Rev. C **73**, 015804 (2006).

[41] T. Rauscher, G. G. Kiss, G. Gyürky, A. Simon, Z. Fülöp, and E. Somorjai, Phys. Rev. C **80**, 035801 (2009).

[42] N. Özkan, G. Efe, R. T. Güray, A. Palumbo, J. Görres, H.-Y. Lee, L. O. Lamm, W. Rapp, E. Stech, M. Wiescher, G. Gyürky, Zs. Fülöp, and E. Somorjai, Phys. Rev. C **75**, 025801 (2007).

[43] http://nucleardata.nuclear.lu.se/toi/.

[44] http://www.isoflex.com/.

[45] http://www.phy.anl.gov/targetlab/index.html.

[46] http://www.srim.org/SRIM/SRIMPICS/STOPPLOTS.htm.

[47] M. Mayer, SIMNRA, http://home.rzg.mpg.de/˜mam/.

[48] C. Iliadis, *Nuclear Physics in Stars* (Wiley-VCH, Berlin, 2007).

[49] C. E. Rolfs and W. S. Rodney, *Cauldrons in the Cosmos* (University of Chicago Press, Chicago, 1988).

[50] C. Yalcin, R. T. Güray, N. Özkan, S. Kutlu, Gy. Gyürky, J. Farkas, G. G. Kiss, Zs. Fülöp, A. Simon, E. Somorjai, and T. Rauscher, Phys. Rev. C **79**, 065801 (2009).

[51] K. Debertin and R. G. Helmer, *Gamma and X-ray Spectrometry with Semiconductor Detectors* (North-Holland, Amsterdam, 1989).

[52] J. P. Biersacke and J. F. Ziegler, SRIM code version SRIM-2008.04.

[53] A. Gilbert and A. G. W. Cameron, Can. J. Phys. **43**, 1446 (1965).

[54] J. P. Jeukenne, A. Lejeune, and C. Mahaux, Phys. Rev. C **16**, 80 (1977).

[55] A. Lejeune, Phys. Rev. C **21**, 1107 (1980).

[56] F.-K. Thielemann and M. Arnould, in *Conference on Nuclear Data for Science and Technology, Antwerp, 6–10 September, 1982*, edited by K. Böckhoff (Reidel, Dordrecht, The Netherlands, 1983), p. 762.

[57] A. J. Koning and J. P. Delaroche, Nucl. Phys. A **713**, 231 (2003).

[58] D. M. Brink, Nucl. Phys. **4**, 215 (1957); P. Axel, Phys. Rev. **126**, 671 (1962).